Polymer Vol. 39 No. 22, pp. 5327–5333, 1998

0032-3861/98/$ - see front matter

PII: S0032-3861(97)10208-7

Isotacticity dependence of spherulitic morphology of isotactic polypropylene

Koji Yamada[a,*], Shimako Matsumoto[a], Katsuharu Tagashira[a] and Masamichi Hikosaka[b]

[a]*Oita Research Center, Japan Polyolefins Co. Ltd., 2 Nakanosu, Oita, 870-0189 Japan*
[b]*Faculty of Intergrated Arts and Sciences, Hiroshima University, 1-7-1 Kagamiyama, Higashi-Hiroshima, 739-8521 Japan*
(Received 13 January 1997; revised 2 October 1997; accepted 13 October 1997)

The isotacticity dependence of the spherulitic morphology of isotactic polypropylene (iPP) with high isotacticity between 98.9% and 99.8% in isotactic pentad fraction ([mmmm]%) was studied. Conventional iPP with low isotacticity, [mmmm] = 93.5%, was used as a reference. Isothermal crystallization was carried out at 125°C–150°C. Morphological observations were carried out by polarizing optical microscopy and transmission electron microscopy. Nearly all the spherulites showed an α-form crystal structure and negative birefringence (Δn). The radial lamellar (R-lamellar) fraction, f_R, estimated from Δn increased with increase in isotacticity and crystallization temperature. This result indicates that the degree of cross-hatching composed of R-lamellae and tangential lamellae (T-lamellae) decreased with increase in isotacticity and crystallization temperature. It was shown for the first time that the spherulite fully occupied by R-lamella, i.e., $f_R \approx 1$, was obtained when the sample with the highest isotacticity was crystallized at 150°C. This means that there are few cross-hatched lamellae. The origin of cross-hatching is discussed, focusing on the role of configurational defects within a molecular chain and the mobility of molecules in the crystallization process.

(Keywords: isotacticity; spherulite; morphology; isotactic polypropylene)

INTRODUCTION

The isotacticity of isotactic polypropylene (iPP) plays an important role in the crystallization process. Until recently, isotacticity has not been sufficiently high, which means that the degree of crystallinity of iPP was not high enough under the usual molding conditions and that iPP could not achieve its ideal physical performances (its mechanical and thermal properties, etc.). Recently, it became possible to obtain iPP with high isotacticity by the development of catalyst technology, so it is expected that the structure and properties of iPP will be improved.

It is well known that there are four polymorphs of iPP: the monoclinic (α), pseudo-hexagonal (β), orthorhombic (γ) and smectic forms[1–5]. Morphologies of the α and β forms are usually spherulitic, in the case of melt crystallization. Spherulitic morphology has been studied extensively for long time. Padden and Keith[6] observed the α- and β-form spherulites by means of polarizing optical microscopy, and classified them into four categories, type I to IV. Types I and II and their mixed type are spherulites of α form, and type III and IV are those of β form. Type I spherulites show positive birefringence (Δn) and appear at a lower crystallization temperatures (T_c) below 134°C, while type II spherulites show negative birefringence and appear at higher T_c, values above 138°C. Under atmospheric pressure, the α-form crystal is the most stable[6]. In the application of iPP to materials for commercial products, the α form is more suitable than the β form because of its higher modulus and thermal resistance. Therefore, we studied only the α-form spherulite in this research.

Observations of the spherulitic and lamellar morphology of iPP were carried out by optical microscopy and by transmission electron microscopy, using the permanganic etching technique[7–9]. It has been found that there are cross-hatched lamellar textures in the interior of a melt-grown α-form spherulite. A similar cross-hatched structure was observed by Khoury[10] for a solution-grown crystal, and it is believed that the morphology of cross-hatching is common for α-form spherulites. Cross-hatching within a spherulite is composed of radial lamellae (R-lamellae) growing along the radius of the spherulite, and tangential lamellae (T-lamellae) crossing nearly orthogonally to the R-lamellae. *Figure 1*(*a*) illustrates the R- and T-lamellae within a two-dimensional spherulite, which is known to be formed in a thin film. The growth direction of the R-lamellae corresponds to the a^* axis in a monoclinic unit cell[11]. It is considered that lateral growth rate along the a^* axis (V_{a^*}) is much larger than that along the *b*-axis (V_b). *Figure 1*(*b*) is an enlarged illustration of the crossing of R- and T-lamellae. In *Figure 1*(*b*), configurational defects (opposite monomer insertions) are shown by filled circles. *Figure 1*(*b*) shows the model of the onset of T-lamellae, which will be discussed in detail below. Type I spherulites show a typical cross-hatched morphology, while in type 2 spherulites, the major portion is composed of R-lamellae. Lotz *et al.*[12–14] proposed that the cross-hatched structure is formed via an epitaxial growth mechanism, showing that the observed crossing angle, 99° 20′, is just the same as the β angle of the monoclinic unit cell of the α form. They suggested that T-lamellae nucleate and grow epitaxially on R-lamellae.

* To whom correspondence should be addressed. Tel: 0975-21-0975; fax: 0975-23-3691; e-mail: yamada@orc.jpo.co.jp

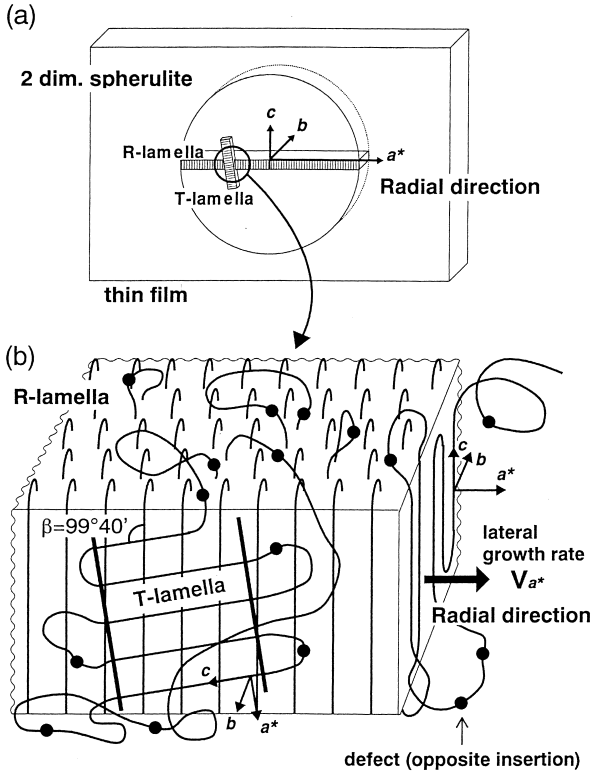

Figure 1 (a) Schematic illustration of a two-dimensional α-form spherulite showing an edge-on lamella. (b) Represention of the onset of a T-lamella growing epitaxially on the side surface of an R-lamella. It is to be noted that the folding direction shown schematically is not real

Binsbergen and Lange[15] proposed a method to estimate the R-lamellar fraction, f_R, using the birefringence (Δn) for a two-dimensional iPP spherulite which is usually seen within a thin film. Awaya[16–18] estimated f_R using their method and the refractive indices along the a^*, b and c axes measured by Takahara *et al.*[19] Δn becomes negative when f_R increases above 0.665 with the increase in T_c. The highest f_R observed by Awaya[16] was 0.71, which means that there are still a lot of T-lamellae in a spherulite.

The isotactic pentad fraction ([mmmm]%) is the most common parameter with which measure isotacticity[20]. In this study, we also used another parameter, the number-average sequence length of meso addition (N_m)[21]. Nm, which will be explained in detail in the experimental section below, is particularly sensitive in the high isotacticity region. Cheng and coworkers studied the effect of isotacticity on the crystallization and melting behaviour of iPP[22–24]. The [mmmm]% and N_m of iPP used in their studies are lower than 98.8% and 500, respectively. The study of iPP of much higher isotacticity has not been reported so far. Cheng *et al.* showed that configurational defects are involved within lamellae when iPP with rather low tacticity is crystallized at rather lower T_c[22], which can be explained by a well-known uniform inclusion model proposed by Sanchez and Eby for random stereo-copolymers[25]. They also showed that the possibility of inclusion of configurational defects decreases with increase in tacticity and T_c. This trend can also be recognized in table 2 of Ref. 22 where the decrease in the amorphous layer thickness between lamellae with an increase in isotacticity is more dominant than the increase in lamellar thickness. These results suggest that configurational defects tend to be excluded from lamellae and are mainly involved in the amorphous region with an increase in tacticity and T_c because the size of the configurational defect is too big to be involved in compactly packed α-form lamella.

It is expected that there is a possibility of formation of a spherulite composed of only defectless R-lamellae when the tacticity and T_c increase. The purpose of this study is to show that a nearly ''perfect'' α-form spherulite, which is composed of only R-lamellae without any T-lamellae and defects within a lamella, will be formed when iPP with very high isotacticity, such as [mmmm] higher than 99.8% and Nm $>$ 2068, is crystallized at a high T_c, higher than 150°C. This study will make clear the important role of tacticity in the formation mechanism of a superstructure, such as T-lamellae and spherulites, of stereo-regular chain polymer materials. This role is still an unsolved important problem in the crystallization of polymers.

EXPERIMENTAL

Samples

Three kinds of high isotacticity temperature-rising elution fractionation (t.r.e.f.) fractions of iPP were used in this study: iPP-A, -B and -C. Their original samples were polymerized with $MgCl_2$-supported catalysts. For comparison, conventional low isotacticty iPP (iPP-D) polymerized with Ziegler–Natta Catalyst was also used. All the samples were stabilized by adding antioxidants, 0.10% of Irganox1010 and 0.15% of Irgafos168 (Ciba-Geigy, Switzerland). Characterizations of the molecular structure of the samples were carried out using ^{13}C nuclear magnetic resonance (^{13}C-n.m.r.) and gel permeation chromatography (GPC) (*Table 1*). The three fractionated samples iPP-A, -B and -C have almost similar molecular weights (Mn = 45–61 $\times 10^3$) and narrow molecular weight distribution (M_w/M_n = 2.1–2.6). The isotacticity of iPP-A is the highest ([mmmm] = 99.8% and N_m = 2068). The isotacticity of iPP-B is in the middle ([mmmm] = 99.6% and N_m = 1209) and that of iPP-C is rather low ([mmmm] = 98.9% and N_m = 434). iPP-D ($M_n = 53 \times 10^3$ and M_w/M_n = 7.6) was used as a reference of typical conventional iPP with the lowest isotacticity ([mmmm] = 93.5% and N_m = 73).

Number-average sequence length of meso addition (N_m)

iPP polymerized with the $MgCl_2$-supported catalyst has only meso or racemic sequences and no head-to-head or 1,3-combination. Therefore, the type of structural defect is only an opposite insertion of monomer. The number-average sequence length of meso addition (N_m) is the average number of monomer units between two opposite insertions of monomer, which is defined by the following equation[21]

$$N_m = \frac{2(\text{mmmm} + \text{mmmr} + \text{rmmr}) + (\text{mmrm} + \text{mmrr} + \text{mrmr} + \text{rmrr})}{\text{mmrm} + \text{mmrr} + \text{mrmr} + \text{rmrr}} \quad (1)$$

Table 1 Molecular characteristics of iPP

	[mmmm] %	N_m [a]	$M_n \times 10^{-3}$	$M_w \times 10^{-3}$	M_w/M_n
iPP-A	99.8	2068	58	137	2.4
iPP-B	99.6	1209	61	130	2.1
iPP-C	98.9	434	45	117	2.6
iPP-D	93.5	73	53	401	7.6

[a]Number-average sequence length of meso addition[21].

Nm was estimated using ^{13}C-n.m.r. signals. If it is assumed that opposite insertions of monomer are included randomly in a molecular chain, the correspondence between [mmmm]% and N_m is approximately given by the following equation

$$N_m \simeq \frac{500}{100 - [\text{mmmm}]\%} \tag{2}$$

Since the portion of the opposite insertion of monomer tends to be excluded from a lamellar crystal due to the size of the configurational defect being too large to be involved in compactly packed α-form lamellae, N_m strongly affects the crystallization behavior of iPP.

Isothermal crystallization

Isothermal crystallization was performed as follows. Films about 15 μm in thickness were prepared using a hot press. The films placed between glass slides were melted in a silicon oil bath at 230°C for 10 min, and then rapidly transferred to another oil bath kept at a chosen T_c between 125°C and 150°C. After the completion of crystallization, they were quenched in ice water.

Morphology

Polarizing optical microscopy. Spherulitic morphology was observed using an OLYMPUS polarizing optical microscope with a sensitive colour plate. The α- and β-form spherulites can easily be distinguished by the observation with the optical microscope. Path differences were measured by using a Berek compensator. Binsbergen and Lange[15] presented a formula to estimate the R-lamellar fraction f_R

$$f_R = \frac{2\Delta n + (n_{a^*} + n_b - 2n_c)}{3(n_{a^*} - n_c)} \tag{3}$$

where n_{a^*}, n_b and n_c are the refractive indices for an α-form crystal along the a^*, b, and c axes, respectively. It is to be noted that equation (3) is formulated for a two-dimensional spherulite with biaxial orientation (a^* and c). Equation (3) can be used for the case of a relatively large f_R, where almost all lamellae are edge-on[18]. In the case of a comparatively small f_R, birefringence approaches zero, because of the existence of edge-on T-lamellae with positive birefringence and flat-on lamellae with little birefringence.

The values of each refractive index were given by Takahara *et al.*[19]

$$n_{a^*} = 1.5067,\ n_b = 1.5070 \text{ and } n_c = 1.5419 \tag{4}$$

Awaya[16–18] obtained the following relationship from equations (3) and (4)

$$f_R = \frac{0.0351 - \Delta n}{0.0528} \tag{5}$$

Transmission electron microscopy (TEM). The permanganic etching technique developed by Bassett *et al.*[7,8] was applied to the present study. The isothermally crystallized thin film was etched for 15 min with the etching reagent prepared by dissolving 0.2 wt% potassium permanganate in 8:2 concentration of sulphuric acid:phosphoric acid mixture in a ultrasonic bath at room temperature. After the treatment, the specimen was washed with a dilute sulphuric acid, hydrogen peroxide, water, and acetone, respectively each for 90 s in an ultrasonic bath. Then, it was dried in a vacuum oven for 1 h at 40°C. The specimen surface was replicated as follows. The surface was coated by carbon vertically after shadowing with platinum/palladium at an angle of 40°. A small amount of 25% polyacrylic acid solution was deposited onto the coated specimen and dried for about 12 h at room temperature. The dried polyacrylic acid layer with the carbon replica is easily removed from a specimen. The polyacrylic acid is dissolved in water for a few hours. The obtained replica is mounted on a grid for TEM observation. TEM observation was performed using a HITACHI H-800 with 100 kV accelerating voltage.

Differential scanning calorimetry (DSC)

DSC measurements were carried out on a Perkin-Elmer DSC7 on isothermally crystallized samples. It was calibrated by the melting temperatures of indium (156.60°C)

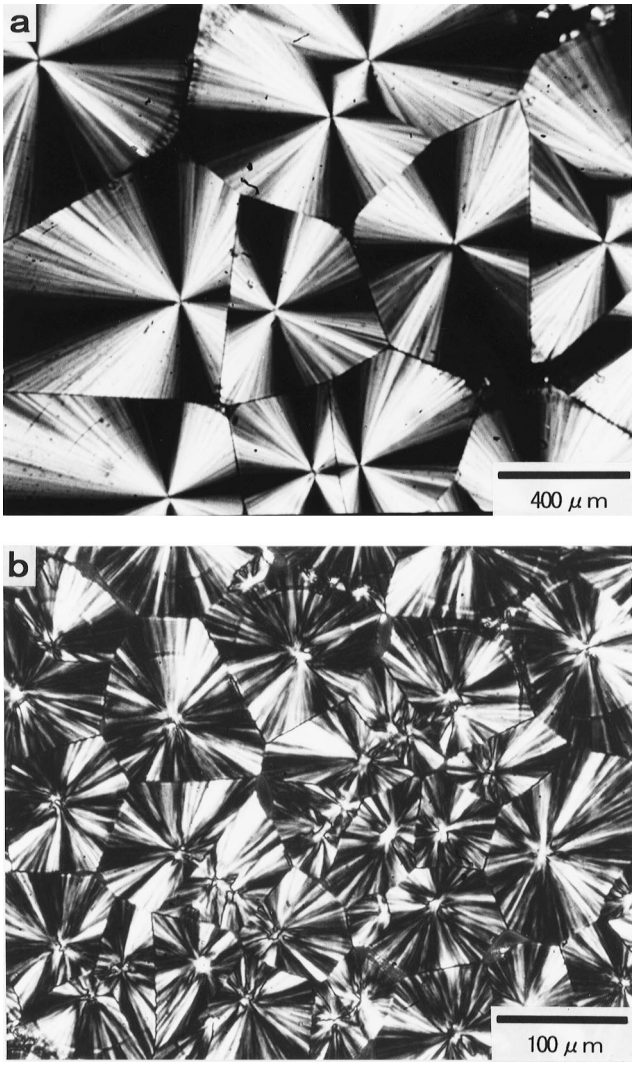

Figure 2 Typical spherulitic morphology observed by polarizing opical microscopy. (a) iPP-A with highest Nm = 2068 crystallized at the highest T_c = 150°C shows an evident Maltese cross, (b) iPP-C with lower N_m = 434 crystallized at the lowest T_c = 125°C shows irregular pattern

and lead (327.45°C) as standards. Each sample was heated from 30°C to 230°C at a rate of 10°C min^{-1} in a nitrogen atmosphere.

RESULTS

Morphology

Typical optical micrographs of spherulites are shown in *Figure 2*. All the spherulites of fractionated samples showed negative birefringence (Type II). For the sample of iPP-A with the highest N_m (= 2068) crystallized at the highest T_c (=150°C), the spherulite shows a pronounced Maltese Cross and a continuous sheaf-like texture aligning radially (*Figure 2*(*a*)), which suggests that R-lamellae are dominant in this spherulite. In contrast, for iPP-C with rather low N_m (=434) crystallized at the lowest T_c (=125°C), the spherulites showed a somewhat distorted Maltese cross (*Figure 2*(*b*)), which suggests that the fraction of T-lamellae increases with decrease in N_m and T_c. Continuous change in spherulitic morphology was observed from (a) to (b) with decrease in N_m and T_c.

Typical transmission electromicrographs of iPP-A crystallized at 150°C and iPP-C crystallized at 125°C are shown in *Figure 3*, where (*a*) and (*b*) correspond to (*a*) and (*b*) of *Figure 2*, respectively. Continuous change in lamellar texture was observed from (*a*) to (*b*) with decrease in N_m and T_c. It is confirmed that a spherulite of the former was composed of almost all radially oriented stacked R-lamellae (*Figure 3*(*a*)), the thickness of which was about 45 nm. In a spherulite of the latter, many T-lamellae are observed between the R-lamellae (*Figure 3*(*b*)), which has a typical cross-hatching structure. The typical thickness of R-lamellae and T-lamellae is about 29 nm and about 21 nm, respectively, i.e. the R-lamellae were thicker than the T-lamellae. Thus it is shown that the fraction and the thickness of the R-lamellae increased with increase in Nm and T_c.

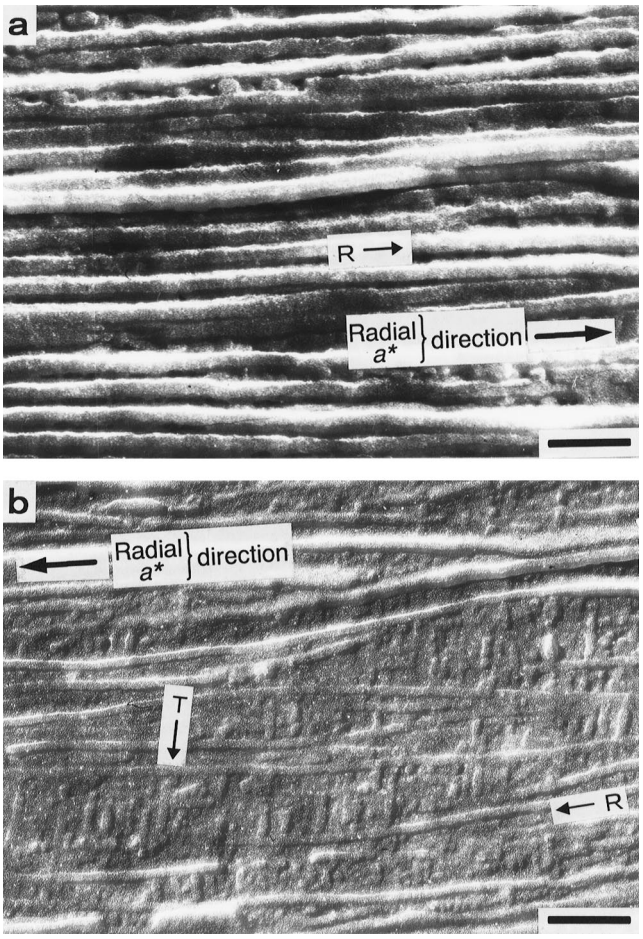

Figure 3 Typical lamellar morphology in iPP spherulites observed by transmission electron microscopy. R and T indicate R-lamella and T-lamella, respectively. The radial direction corresponds to the a^* direction of an α-form unit cell. (a) Stacked R-lamellae for iPP-A (N_m = 2068) crystallized at 150°C; (b) cross-hatched lamellae for iPP-C (N_m = 434) crystallized at 125°C. Sclae bar = 0.2 μm

DSC

Typical melting behaviours observed by DSC for isothermally crystallized specimens are shown in *Figure 4*(*a*) and (*b*), corresponding to (*a*) and (*b*) of *Figure 2* and *Figure 3*, respectively. Continuous change was observed from (a) to (b) with decrease in N_m and T_c. It is reported that the melting temperature (T_m) of β-form crystals is 152°C, while that of α-form crystals is higher than 160°C[5]. For iPP-A crystallized at high T_c (=150°C), melting endotherm peaks of the α-form crystals at 171.8°C and 179.7°C, higher than 160°C, were observed (*Figure 4*(*a*)). For iPP-C crystallized at rather low T_c (=125°C), dominant melting peaks of the α-form crystal at 164.0°C and a small melting peak of the β-form crystal at 150.2°C were observed (*Figure 4*(*b*)). It was confirmed that all the spherulites observed in the present study were mainly composed of α-form crystals. T_m increased with increase in N_m and T_c. These melting behaviours were in good agreement with the microscopic observations.

R-lamellar fraction, f_R

The R-lamellar fraction, f_R, estimated using equation (5), is plotted against T_c for three kinds of specimens, iPP-A, -B and -C (*Figure 5*). f_R increased with increase in T_c for all the samples. f_R also increased with the increase in isotacticity. For iPP-A with the largest N_m crystallized at the highest T_c (=150°C), f_R reaches nearly 1. It should be stressed that a nearly ''perfect'' α-form spherulite composed of only R-lamellae was obtained for the first time. For iPP-C with

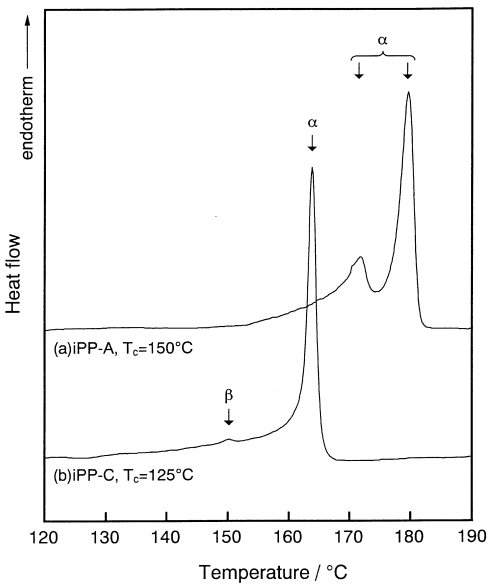

Figure 4 Typical DSC melting behaviours of samples iPP-A and -C crystallized isothermally at (a) 150°C for 48 h, and (b) 125°C for 15 min

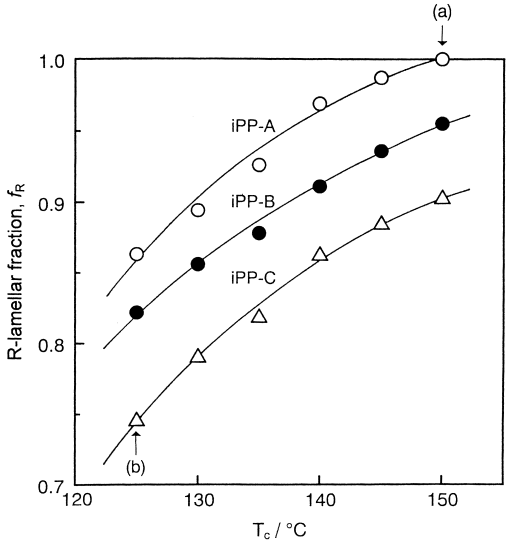

Figure 5 Plot of R-lamellar fraction f_R against crystallization temperature T_c: ○, iPP-A; ●, iPP-B; △, iPP-C. (a) and (b) indicated by arrows correspond to (a) and (b) of *Figure 3*, respectively

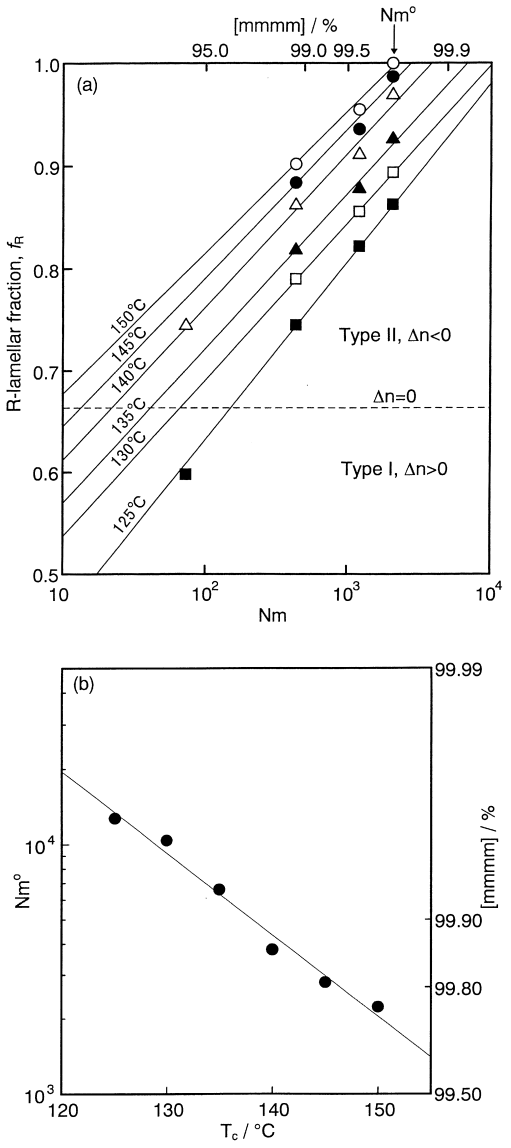

Figure 6 (a) Plot of R-lamellar fraction f_R against Nm or [mmmm}. Dotted line corresponds to f_R for $\Delta n = 0$. Nm° is Nm for $f_R = 1$. Arrow indicates Nm° for $T_c = 150$°C. (b) Plot of Nm° against T_c obtained from (a)

lower Nm crystallized at lower T_c (= 125°C), in contrast, f_R is about 0.75, which means that the fraction of T-lamellae is about 0.25. Thus it was confirmed qualitatively that f_R increases with the increase in N_m and T_c.

Isotacticity dependence of f_R

The relationship between Nm and f_R is much more clearly shown in *Figure 6*(a). Another isotacticity parameter of [mmmm] is also shown in the upper horizontal axis. f_R increased linearly with increase in log N_m, from which the following experimental formula was obtained

$$f_R = A \log N_m + B \quad (6)$$

where A and B are constants. A decreased from 0.18 to 0.14 (1/log N_m) and B increased from 0.26 to 0.53 with increase in T_c. Here we will denote N_m for $f_R = 1$ as $N_m°$. $N_m°$ was estimated to be 2000 for $T_c = 150$°C. This indicates that an almost ''perfect'' α-form spherulite was obtained for the first time. It is easy to estimate the $N_m°$ from the point in *Figure 6*(*a*) where f_R reaches 1. The log $N_m°$ is plotted against T_c in *Figure 6*(*b*). log $N_m°$ decreased linearly with T_c, that is

$$\log N_m° = C - \Delta T_c \quad (7)$$

where C and D are constants, $C = 17.14$ and $D = 0.033$ (1/K). It is predicted that the ''perfect'' α-form spherulite will be obtained even when iPP is crystallized at lower T_c, such as below 140°C, if very pure iPP, such as [mmmm] > 99.9%, could be crystallized. This also means that a ''perfect'' α-form spherulite can be obtained even for iPP with lower N_m if it could be crystallized at higher T_c.

For the conventional iPP with the lowest N_m (iPP-D, $N_m = 73$), the spherulite shows positive birefringence for $T_c = 125$°C and negative birefringence for $T_c = 140$°C. For iPP-D, the transition temperature of the α-form spherulitic morphology from type I to type II was about 130°C which agrees well with Padden and Keith's[6] and Norton and Keller's[9] results, 134–138°C.

DISCUSSION

Formation mechanism of T-lamellae

It is well known that the α-form iPP crystals form a cross-hatched lamellar structure which is composed of R- and T-lamellae. The present study showed that the fraction of T-lamellae (i.e. cross-hatching) decreased to zero as isotacticity (N_m) and T_c significantly increased. The isotacticities of iPPs reported[10,12–15] so far were lower than those of the iPPs used in this study. Therefore, the formation of T-lamellae should be strongly related to configurational defects within a molecular chain (opposite insertion of monomer) and the decrease in diffusion (mobility) of chain molecules necessary for crystallization.

The morphological characteristics and the origin of T-lamellae have been extensively studied[10,12–15]. It has been established that a T-lamella subsidiary nucleates epitaxially on the side surface (010) of an R-lamella by a satisfactory interdigitation of the methyl groups of the facing plane[12–14]. The rate of epitaxial nucleation of T-lamellae depends on the degree of supercooling[15]. Therefore, the R- and T-lamellae are often called mother- and daughter-lamellae, respectively. Thus the formation of the T-lamellae has been regarded as the process of secondary crystallization.

Here we will present a schematic model of the onset of T-lamellae and show that a long loose loop will easily nucleate epitaxially on the side surface, which is the

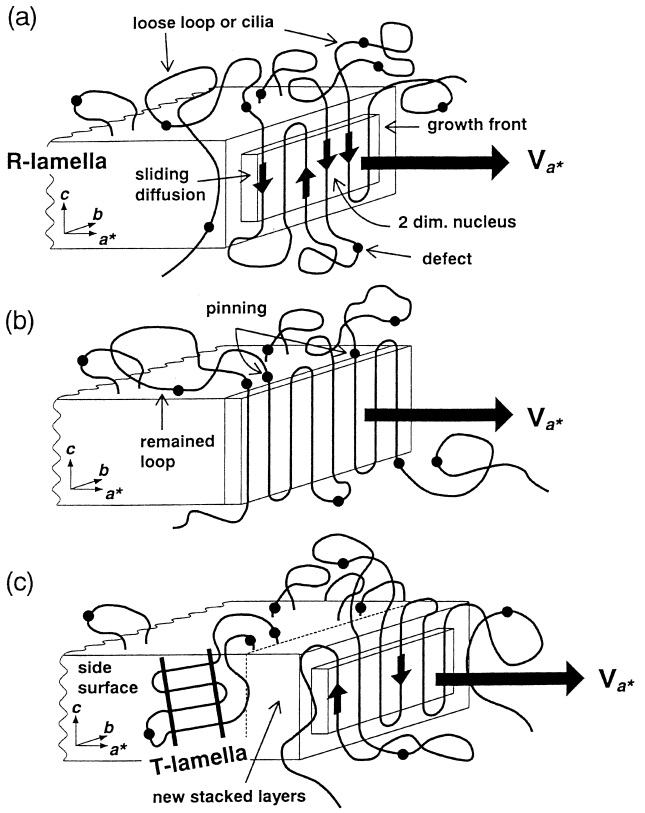

Figure 7 Schematic representation of the formation process of a T-lamella. (a) A nucleus formed on the growth front of a lamella grows via a pulling-in of loose loops or cilia, (b) the pulling-in stops by pinning due to a defect in molecule or the stacking of layers on the nucleus, (c) epitaxial nucleation of the loop on the side surface (010) of an R-lamella which forms a T-lamella

origin of T-lamellae. *Figure 7* schematically represent a model to explain the formation mechanism of T-lamellae. *Figure 7*(*a*) illustrates a chain which is partially crystallized on the growth front forming a two-dimensional nucleus (2-dim. nucleus) and which partially remained within the melt, forming loose loops or cilia. In the two-dimensional nucleation and growth and lamellar thickening processes, the loose loops or cilia should be pulled into the nucleus via chain sliding diffusion[26,27].

The pulling in and sliding diffusion of a molecule will be slowed down or nearly stopped when a defect (the opposite insertion of monomer) reaches the end surface of the nucleus (*Figure 7*(*b*)) or a new nucleus is stacked on the present nucleus, forming stacked layers on the growth front (*Figure 7*(*c*)), because the size of the defect is so large that it cannot easily be inserted within the crystalline lattice, and the stacked layers strongly suppress the sliding diffusion of chains. In this case, the long loops or cilia will remain within the melt (*Figure 7*(*b*)). The position of the remaining loops or cilia will be limited around that of the pinning points. Therefore, the possibility for loops or cilia to attach onto the side surface and nucleate epitaxially near the pinning points and grow into the T-lamellae is higher than that for free molecules within the melt (*Figure 7*(*c*)). The model of the onset of T-lamellae explains well the observed results that the fraction of T-lamellae increased with decrease in Nm and T_c. This means that the T-lamellae are formed by a overgrowth process, i.e. secondary nucleation, as has been reported. It has been known that the thickness of R-lamellae is larger than that of T-lamellae, which may be due to the fact that molecules within the T-lamellae include a higher density of defects, which will slow down the lamellar thickening as mentioned above, than those of R-lamellae. Thus it is expected that the degree of crystallinity which relates to the mechanical and thermal properties will be improved for iPP with a decrease in configurational defects.

CONCLUSION

1. The fraction of the amount of cross-hatched lamellar texture of iPP decreased with the increase in isotacticity (Nm) and crystallization temperature (T_c), where Nm is the number-average sequence length of meso addition. The cross-hatched lamellae are composed of radial lamellae (R-lamellae) and tangential lamellae (T-lamellae). The R-lamellar fraction (f_R) was estimated by the birefringence measurement. It was shown for the first time that $f_R = 1.0$ when N_m and T_c increased up to 2068 and 150°C, respectively, which means that there are almost no cross-hatched lamellae.
2. R-lamellae were shown to be thicker than T-lamellae, therefore it is expected that heat resistance will be improved with increase in f_R. The degree of crystallinity of iPP generally increases with the increase in T_c. Therefore, it can be expected that thermal and mechanical properties will be improved by controlling N_m and T_c.
3. The formation mechanism of the T-lamellae, i.e. the cross-hatched lamellae of iPP spherulite, is proposed. When Nm and T_c are low, it is expected that long loops or cilia will remain on the end surface of lamellae during the surface nucleation and growth process. This is because pinning of so-called refolding would occur, when molecular defects attach to the end surface, which is due to the fact that the defect is too large to be included within the lamellae. The loops or cilia will form the T-lamellae via epitaxial growth on the side surface. This model explains the observed facts well.[23,24]

ACKNOWLEDGEMENTS

This work was partly supported by a Grant-in-Aid for Scientific research (B), No.07455386 and an International Joint Research Grant, NEDO, 1996–1998. Fruitful discussion with Dr. Tadao Suzuki, consultant of Shows Denko K.K., is gratefully acknowledged.

REFERENCES

1. Natta, G. and Corradini, P., *Nuovo Cim. Supp.*, 1960, **15**, 1.
2. Keith, H. D., Padden, F. J., Walter, N. M. and Wycoff, M. W., *Appl. Phys.*, 1959, **30**, 1485.
3. Bruckner, S. and Meille, S. V., *Nature*, 1989, **340**, 455.
4. Samuels, R. J., and Yee, R. Y., *J. Polym. Sci., A-2*, 1972, **10**, 385.
5. Varga, J., *J. Mater.,Sci.*, 1992, **27**, 2557.
6. Padden, F. J. and Keith, H. D., *J. Appl. Phys.*, 1959, **30**, 1479.
7. Bassett, D. C. and Olley, R. H., *Polymer*, 1984, **25**, 935.
8. Bassett, D. C. and Olley, R. H., *Polymer*, 1989, **30**, 399.
9. Norton, D. R. and Keller, A., *Polymer*, 1985, **26**, 704.
10. Khoury, F. A., *J. Res. Natl. Bur. Std.*, 1966, **70A**, 29.
11. Kojima, H., *J. Polym. Sci. A-2*, 1967, **5**, 597.
12. Lotz, B., Wittmann, J. C. and Lovinger, A. J., *Polymer*, 1996, **37**, 4979.
13. Lotz, B. and Wittmann, J. C., *J. Polym. Sci. B. Polym. Phys.*, 1986, **24**, 1541.
14. Stocker, W., Magonov, S. N., Cantow, H.-J., Wittmann, J. C. and Lotz, B., *Macromolecules*, 1993, **26**, 5915.

15. Binsbergen, F. L. and de Lange, B. G. M., *Polymer*, 1968, **9**, 23.
16. Awaya, H., *Koubunshi Kagaku*, 1972, **29**, 322.
17. Awaya, H., *Polymer*, 1988, **29**, 591.
18. Awaya, H., *Seikei-Kakou*, 1996, **8**, 537.
19. Takahara, H., Kawai, H. and Yamada, T., *Seni-Gakkaishi*, 1962, **23**, 571.
20. Cheng, H. N., *J. Appl. Polym. Sci.*, 1988, **35**, 1639.
21. Randall, J. C., *Polymer Sequence Determination*, Academic Press, 1977, Chap. 2, pp. 29-40.
22. Cheng, S. Z. D., Janimak, J. J., Zhang, A. and Hsieh, E. T., *Polymer*, 1991, **32**, 648.
23. Janimak, J. J., Cheng, S. Z. D., Giusti, P. A. and Hsieh, E. T., *Macromolecules*, 1991, **24**, 2253.
24. Janimak, J. J., Cheng, S. Z. D., Zhang, A. and Hsieh, E. T., *Polymer*, 1992, **33**, 728.
25. Sanchez, I. C. and Eby, R. K., *J. Res. Natl. Bur. Std. (A)*, 1973, **77**, 353.
26. Hikosaka, M., *Polymer*, 1987, **28**, 1257.
27. Hikosaka, M., *Polymer*, 1990, **31**, 458.